JAAS

PAPER

View Article Online
View Journal | View Issue

Cite this: J. Anal. At. Spectrom., 2016, 31, 658

High-precision zircon U/Pb geochronology by ID-TIMS using new 10^{13} ohm resistors†

Albrecht von Quadt,*[a] Jörn-Frederik Wotzlaw,[a] Yannick Buret,[a] Simon J. E. Large,[a] Irena Peytcheva[ab] and Anne Trinquier[c]

Accessory mineral U–Pb geochronology by isotope dilution thermal ionization mass spectrometry (ID-TIMS) requires precise and accurate determinations of parent–daughter isotope ratios. The small sample size, particularly with respect to radiogenic Pb (Pb*), requires highly sensitive ion detection systems. Most studies therefore employ either secondary electron multipliers (SEMs) or Daly photomultipliers that provide low background noise and high sensitivity but have a limited linear range and require dynamic peak-hopping. We here evaluate the application of new 10^{13} ohm resistors in a Faraday cup amplifier feedback loop for the static collection of all Pb isotopes (sample and tracer) with ^{202,205,206,207,208}Pb measured on Faraday cups and ^{204}Pb measured in the axial SEM of a Thermo Scientific™ TRITON™ Plus TIMS instrument. We demonstrate long-term stability of the amplifier gain calibration using a secondary Nd standard and test short- and long-term stability and reproducibility of amplifier baselines. Accurate calibration of static detector arrays is demonstrated by repeated analyses of synthetic and natural U–Pb standards (ET100, Temora-2 and AUS_Z7_5) with variable Pb* (0.551 to 699 pg) and comparison with conventional dynamic ion counting data. Excellent agreement between the two detector systems for all analysed standards suggests that our static measurement routine with 10^{13} ohm resistors produces accurate and precise U–Pb isotopic data with superior external reproducibility. We anticipate that this new technique will push the frontiers of high-precision U–Pb geochronology and may represent a crucial advancement in the quest towards inter- and intra-laboratory reproducibility at the 0.01% level.

Received 18th November 2015
Accepted 15th December 2015

DOI: 10.1039/c5ja00457h

www.rsc.org/jaas

Introduction

U–Pb geochronology by isotope dilution thermal ionization mass spectrometry (ID-TIMS) is the most precise and most accurately calibrated method for the determination of crystallization ages of accessory minerals.[1] Precise and accurate analyses of Pb/Pb and U/Pb (*i.e.*, parent–daughter) isotopic ratios are required to obtain useful age information. The minerals selected for analyses are usually small (~100–500 μm) and contain small amounts of radiogenic Pb (<1 pg to ~1 ng), making the mass spectrometry particularly difficult. The main factors limiting the precision and accuracy of U–Pb isotopic analyses of such small samples are (1) uncertainties associated with the correction for laboratory contamination derived common Pb, (2) corrections for instrumental mass fractionation during analysis and (3) various instrumental parameters affecting the precision and accuracy of isotope ratio measurements (detector sensitivity and linearity, ionization efficiency, *etc.*). The impact of the laboratory blank correction can be minimized through advanced clean laboratory procedures that yield total procedural Pb blanks as low as ~0.2 pg. Mass fractionation correction is more complex because none of the isotopic ratios are constant in natural Pb and natural U only has two long-lived isotopes. Therefore, mass fractionation cannot be corrected by internal normalization. However, isotope dilution using a tracer solution with two Pb isotopes not present in natural Pb (^{202}Pb and ^{205}Pb) as well as two U isotopes of which at least one is not present in natural U (^{233}U) provides a means for real-time mass fractionation correction.[2,3] A newly mixed double-Pb and double-U tracer solution that was prepared, calibrated and distributed as part of the EARTHTIME initiative[3,4] (http://www.earth-time.org) contains the artificial isotopes ^{202}Pb and ^{205}Pb as well as ^{233}U and ^{235}U (ET2535). This allows for real-time mass fractionation correction, leading to highly precise and accurate determinations of the Pb isotopic composition and U/Pb isotopic ratios. The most accurate and precise technique for these analyses is TIMS due to efficient ionization and high ion yields as well as long-lasting and stable ion beams allowing data acquisition over several hours. Most previous studies employed ion counting systems (secondary electron multipliers or Daly photomultipliers) to measure the Pb isotopic composition due to the small amounts of radiogenic

[a]Department of Earth Sciences, Institute of Geochemistry and Petrology, ETH Zurich, Switzerland. E-mail: vonquadt@erdw.ethz.ch

[b]Bulgarian Academy of Science, Geological Institute, Sofia, Bulgaria

[c]Thermo Fisher Scientific, Bremen, Germany

† Electronic supplementary information (ESI) available: Table S1. See DOI: 10.1039/c5ja00457h

Pb in single accessory minerals.[5–7] These studies demonstrate the potential of obtaining single zircon dates with precision and accuracy at the 0.05% level. In this paper, we investigate the use of Faraday cup amplifiers connected with state-of-the-art 10^{13} ohm resistors in the feedback loop for the static collection of small radiogenic Pb ion beams.

Compared to 10^{11} ohm resistors, the use of 10^{13} ohm resistors results in a 100 times higher signal intensity while the noise only increases by a factor of $\sqrt{100}$ (Johnson–Nyquist noise), and thus a tenfold improvement in the signal to noise ratio.[8] This allows for the measurement of ion currents that are in the range normally only covered by ion counting systems. Thereby these measurements take advantage of the superior stability of Faraday detectors, their significantly larger dynamic range and the multiple advantages of static multi-collector analyses (longer counting on peaks, simultaneous collection of all isotopes, *etc.*). The successful application of multiple 10^{13} ohm resistors has been demonstrated for the measurement of sub-ng Sr, Nd and common Pb samples,[8,9] but has not been investigated previously for small quantities of U (ng) and radiogenic Pb (Pb*; pg) isotopes. Here we present an analytical protocol for the precise measurement of the U/Pb isotopic composition of zircon samples employing these new 10^{13} ohm resistors. The precision and reproducibility of our protocol are evaluated by repeated analyses of the synthetic ET100 U/Pb solution[10] (http://www.earth-time.org) and two natural zircon standards (Temora-2, AUSZ7_5). The accuracy is assessed by comparing these analyses with data obtained by conventional U–Pb analyses using a secondary electron multiplier for the Pb isotope measurement and Faraday cups equipped with 10^{11} ohm resistors for the U isotope measurement.

Experimental

Chemical separation, reagents and blanks

In order to minimize the effects of lead loss, all natural zircon samples were pre-treated using a chemical abrasion (CA) technique.[11] All crystals and crystal fragments were annealed at 900 °C for 48 hours. After annealing, individual crystals or fragments were rinsed in 4 N HNO_3 and transferred into Savillex microcapsules together with 100 μl concentrated HF. The microcapsules were arranged in Parr vessels and zircons were partially dissolved ("chemically abraded") for 15 hours at 180 °C. This technique has been shown to be most effective for removing strongly radiation damaged zircon domains that underwent post-crystallization lead-loss. After the partial dissolution step, the crystals were transferred into 3 ml Savillex beakers and the leachate was completely pipetted out. The remaining zircons were fluxed for several hours in 6 N HCl on a hotplate at ~80 °C and repeatedly ultrasonically cleaned in double-distilled 4 N HNO_3. Single zircons were transferred back into their cleaned microcapsules with a microdrop of 7 N HNO_3 and 70 μl of concentrated HF. Prior to dissolution, samples were spiked with 6–15 mg of the ^{202}Pb–^{205}Pb–^{233}U–^{235}U tracer solution.[3,4] After adding the mixed U/Pb tracer, the microcapsules were arranged back into the Parr vessel and zircons were dissolved for 60 hours at 210 °C. After dissolution, samples were dried down and re-dissolved in 6 N HCl at 180 °C for 12 hours in Parr vessels. Re-dissolved samples were again dried down and taken up in 3 N HCl for column chemistry. Pb and U were separated by anion exchange chromatography in 50 μl microcolumns using HCl based ion exchange chemistry. The U–Pb fractions were loaded with a microdrop of silica gel on zone-refined rhenium filaments that were stepwise outgassed at a current between 2 and 4.5 A at pressure $<2 \times 10^{-7}$ mbar for 4–6 h. Total procedural Pb blanks of this protocol, measured during the course of this study, ranged from 0.08 to 0.34 pg. All common Pb in zircon analyses (0.09 to 0.59 pg) was attributed to laboratory blanks and corrected with the following isotopic composition: $^{206}Pb/^{204}Pb = 18.10 \pm 0.38$, $^{207}Pb/^{204}Pb = 15.35 \pm 0.47$, and $^{208}Pb/^{204}Pb = 38.01 \pm 1.14$ (all 2 SD).

Mass spectrometry

The Thermo Scientific™ TRITON™ Plus instrument at the Institute of Geochemistry and Petrology of ETH Zurich is equipped with 9 Faraday cups, 3 secondary electron multipliers (SEMs), and 3 compact discrete dynodes (CDDs). The Faraday cups can be connected to 10 different current amplifiers through a relay matrix. Five of the current amplifiers installed in our TRITON Plus have conventional 10^{11} ohm resistors, whereas the other 5 amplifiers are equipped with new 10^{13} ohm resistors. Our new protocol includes static Pb and U measurements using Faraday cup configurations and amplifier setups shown in Table 1 and data acquisition parameters given in Table 2. The accuracy, precision and reproducibility of these static measurements are assessed by comparison with U–Pb data acquired using conventional ion counting (MasCom SEM) for the analysis of Pb isotopes and using 10^{11} ohm resistors for the static U measurement.

Table 1 Collector setups used for static analysis of Pb and U isotopes and for the gain calibration protocol (see the text for details)

Cup	L4	L3	L2	L1	C	H1	H2	H3	H4
U–Pb routine									
Amp Pb	10^{11}	10^{11}	10^{11}	10^{13}	SEM	10^{13}	10^{13}	10^{13}	10^{13}
Mass				^{202}Pb	^{204}Pb	^{205}Pb	^{206}Pb	^{207}Pb	^{208}Pb
Amp U	10^{11}	10^{13}	10^{13}	10^{13}	SEM	10^{13}	10^{13}	10^{11}	10^{11}
Mass		$^{265}UO_2$	$^{267}UO_2$	$^{270}UO_2$					
Amp Nd	10^{13}	10^{13}	10^{11}	10^{13}	10^{11}	10^{11}	10^{13}	10^{13}	10^{11}
Mass	^{142}Nd	^{143}Nd	^{144}Nd	^{145}Nd	^{146}Nd	^{147}Sm	^{148}Nd	^{150}Nd	

Table 2 Analytical protocol for the static Pb and U measurements with new 10^{13} ohm amplifiers

Analytical protocol	Pb-runs	U-runs
^{204}Pb	SEM	
^{202,205,206,207,208}Pb, $^{265,267,270}UO_2$	10^{13} Ω	10^{13} Ω
Baseline Faraday cups	900 s at start	900 s at start
Gain calibration	JNdi	JNdi
Data acquisition	20–40 blocks of 10 cycles	10–20 blocks of 10 cycles
Integration time	16 s	16 s
Idle time	4 s	4 s
Run temperature	1180–1250 °C	1350–1420 °C

Static Faraday measurements using 10^{13} ohm resistors

Cup configurations. All Pb and U isotopes were measured in static mode (Table 1). ^{202}Pb, ^{205}Pb, ^{206}Pb, ^{207}Pb and ^{208}Pb were measured on Faraday cups connected to amplifiers with 10^{13} ohm resistors and ^{204}Pb was measured using the axial SEM. This configuration does not allow the measurement of masses 201 and 203 to monitor potential isobaric interferences from $BaPO_2^+$ (m/z = 201 to 205) and Tl^+ (m/z = 203 and 205; see ref. 2 for details). However, we routinely monitor these masses during dynamic SEM Pb measurements and usually detect <300 cps on mass 201 and <1 cps on mass 203 suggesting that these interferences are negligible for all Pb runs. U was measured as UO_2 oxides with all three masses of interest ($^{265}(UO_2)$, $^{267}(UO_2)$ and $^{270}(UO_2)$) collected in Faraday cups connected to amplifiers with 10^{13} ohm resistors.

Gain calibration. Gain calibration factors for the 10^{11} ohm resistors were determined using the regular software controlled gain procedure (3.33333 V on all amplifiers with 10^{11} ohm resistors). This procedure is not implemented for the new 10^{13} ohm resistors.

Instead, the gain calibration factors have to be determined using analyses of a secondary standard. We adopted the gain calibration protocol of ref. 12 that uses the certified Nd standard JNdi-1 to determine gain calibration factors for five amplifiers with 10^{13} resistors simultaneously. The Faraday cup setup for the Nd measurement is shown in Table 1. The Nd isotopes ^{144}Nd and ^{146}Nd are connected to 10^{11} ohm resistors and the ^{146}Nd/^{144}Nd ratio is normalized to 0.7219 to obtain within-run mass fractionation factors. The other five Nd isotopes (^{142}Nd, ^{143}Nd, ^{145}Nd, ^{148}Nd, and ^{150}Nd) are connected to 10^{13} ohm amplifiers. The measured Nd isotopic ratios (^{142}Nd/^{144}Nd, ^{143}Nd/^{144}Nd, ^{145}Nd/^{144}Nd, ^{148}Nd/^{144}Nd, and ^{150}Nd/^{144}Nd) are normalized to the long-term average Nd isotopic ratios measured with 10^{11} ohm amplifiers and the obtained gain factors are manually updated in the system table.

The gain factors of the 10^{13} amplifiers were found to vary by less than 100 ppm (2 SD) by Thermo Fisher Scientific[12] over a period of 6 months. Over the course of this study (~3 months), the gain factors of our amplifiers with 10^{13} ohm resistors varied by between ±66 ppm and ±117 ppm (2 RSD; Fig. 1). We stress that these gain measurements are crucial for the accuracy of

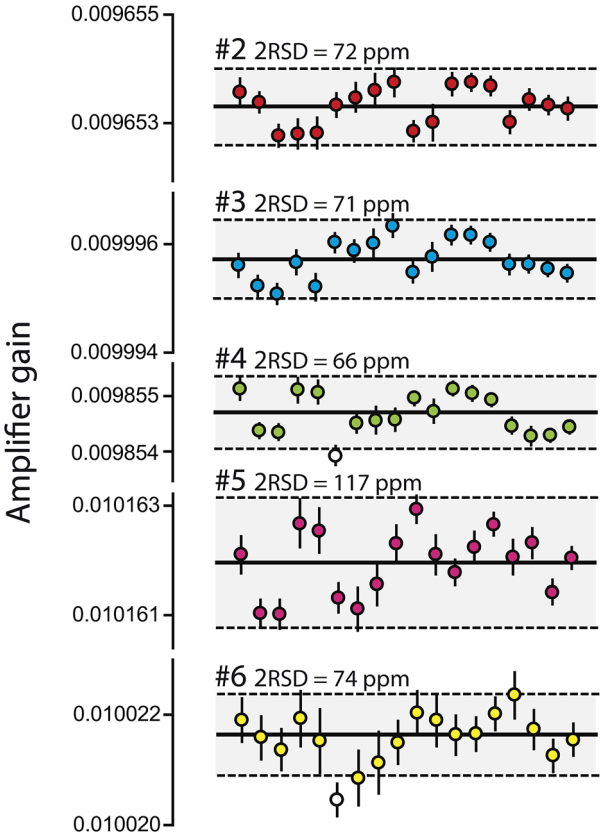

Fig. 1 Reproducibility of the gain calibration factors of the 10^{13} ohm amplifiers as determined through the measurement of the JNdi standard solution over the course of this study. Note that one gain measurement of amplifier #4 and one gain measurement of amplifier #6 were discarded as outliers using 2σ outlier criteria and are shown as open symbols.

subsequent isotope ratio determinations and that they have to be performed with a stable ion beam. We therefore routinely load a new JNdi standard with each series of samples and perform the gain calibration 1–2 times per week. During the gain measurements we carefully monitor the signal intensities and attempt to have less than 5% drift in ion beam intensity over the course of the one hour measurements.

Yield measurements. The ion yield of the SEM system relative to the Faraday cups was determined daily using the NBS 982 standard or a stable sample Pb signal. Yield measurements using stable ^{206}Pb signals with intensities between 6 and 8 mV typically have uncertainties of <0.1% and repeated analyses are reproducible to better than 0.3% over the course of several days at constant SEM operating voltage demonstrating sufficient stability of our SEM system for static mixed Faraday-SEM measurements.

Baselines. Baselines were measured as the average of 900 1.05 s integrations before the Pb isotopic measurements during heating of each sample and after changing the amplifier positions between the Pb and U measurements. Baselines were determined on peaks with the analyser gate closed. During the data collection of Pb and U, no further baseline measurements were carried out. The short term (1 hour) stability

measurements of the 10^{13} ohm amplifiers yielded baseline noise between ±3.1 μV and ±4.8 μV (1 SD; normalized to the 10^{11} ohm resistor gain) on 4 s integrations over a time period of several months (Appendix, Fig. 6) that is within the specification of Thermo Fisher Scientific (<5 μV). This noise level of our 10^{13} ohm resistors is approximately 5 times lower than the noise of the 10^{11} ohm resistors (~20 μV) when both are normalized to the 10^{11} ohm resistor gain (*i.e.*, ~20 times higher when not normalized). This is in agreement with the findings of Koornneef *et al.*[8] but it is a factor of two worse than that predicted by the Johnson–Nyquist equation. We note that the reproducibility of the baseline measurements and the stability of individual baselines were significantly improved by evacuating the amplifier housing using a separate vacuum pump (Fig. 6).

Data reduction, age calculation and uncertainty propagation

Dynamic SEM and static Faraday measurements were corrected for instrumental mass fractionation using the ET2535 double spike. Pb mass fractionation factors were derived from the measured $^{202}Pb/^{205}Pb$ ratio normalized to the true value of 0.99924 (ref. 2). U isotopic ratios were corrected for isobaric interferences of $^{233}U^{18}O^{16}O$ on $^{235}U^{16}O_2$ using an $^{18}O/^{16}O$ of 0.00205 ± 0.000025 and for mass fractionation using the measured $^{233}U/^{235}U$ ratio relative to the true value of 0.99506 (ref. 2) and a sample $^{238}U/^{235}U$ of 137.818 ± 0.045 (ref. 13).

Data reduction was performed using the Tripoli and U–Pb_Redux software package[14] that uses data reduction and uncertainty propagation algorithms of ref. 15. U–Pb ratios and dates were calculated relative to a tracer $^{235}U/^{205}Pb$ ratio of 100.23 ± 0.046% $(2\sigma)^3$ and using the decay constants.[16] All uncertainties are reported at the 2σ level and systematic uncertainties associated with the tracer calibration and decay constants are ignored unless otherwise indicated.

Results and discussion

Synthetic solution ("ET100")

ET100 is a synthetic U–Pb solution prepared and distributed by Daniel J. Condon (British Geological Survey, NERC Isotope Geosciences Facilities, Keyworth, UK) within the framework of the EARTHTIME initiative for inter-laboratory experiments[10] (http://www.earth-time.org). We performed multiple analyses of individual aliquots of this synthetic solution to assess the precision, accuracy and reproducibility of the U/Pb measurements using the static Faraday routine with 10^{13} ohm resistors. A total of 15 aliquots with 47–152 pg Pb* were analysed using conventional dynamic ion counting for the Pb measurements and 15 aliquots with 39–107 pg Pb* were analysed using the static Faraday routine using the 10^{13} ohm resistors (Table S1;† Fig. 2). Analyses with Pb measured on the SEM yielded concordant results with a weighted mean $^{206}Pb/^{238}U$ date of 100.203 ± 0.011 Ma (2σ). Analyses with Pb measured in static mode using 10^{13} ohm resistors also yielded concordant results with a weighted mean $^{206}Pb/^{238}U$ date of 100.189 ± 0.008 Ma. The excellent agreement between the two detector setups suggests accurate calibration of the two systems. However, data with Pb measured on the SEM show excess dispersion in $^{206}Pb/^{238}U$ dates with a MSWD of 5.1 while the static measurements yielded a MSWD of 1.5, indicating no or little excess dispersion (Fig. 2). A better visualization of the difference in data dispersion is shown in Fig. 2 with uncertainties given as (1) two standard errors (2 SE) without taking into account the data dispersion, (2) as the 95% confidence interval that takes into account the data dispersion by expanding the uncertainty by the student's *t*-test multiplied by the square root of the MSWD and (3) as two standard deviations (2 SD) reflecting the reproducibility of the mean values. The precision of individual dates is comparable between the two datasets despite the fact that the within-run precision of the static Pb measurements is up to a factor of 2 more precise than that of the SEM measurements. This is because the dominant source of uncertainty in the final U–Pb date is the uncertainty in the $^{18}O/^{16}O$ ratio used for the U-oxide interference correction (see ref. 15 for details). While the precision of individual $^{206}Pb/^{238}U$ dates is comparable, the static U–Pb measurements display a greater than two-fold improvement in reproducibility relative to dynamic SEM measurements.

Natural zircons

To further test the performance of our static measurement routine in different scenarios, we analysed multiple aliquots of two natural zircon standards (Temora-2, AUS_Z7_5; Fig. 3–5; Table S1†). The selected zircon standards have $^{206}Pb/^{238}U$ ages of 417 Ma and 2.4 Ma and Pb* abundances of 0.5 pg to 700 pg, thus representing end-member scenarios with respect to ion beam intensities (Fig. 5) and sample-spike ratios.

Temora-2. Temora-2 zircon is a widely used standard zircon extracted from the Middledale Gabbroic Diorite (Eastern Australia) and was initially characterised by Black *et al.*[17] Five aliquots containing 137–699 pg Pb* were analysed with Pb measured by dynamic ion counting and five aliquots containing 219–596 pg Pb* were analysed using the static routine with 10^{13} ohm resistors. All analyses from both datasets plot within the uncertainty interval of the concordia (Fig. 3). The five aliquots with Pb measured on the SEM yielded ^{230}Th-corrected $^{206}Pb/^{238}U$ dates between 417.01 ± 0.28 Ma and 417.61 ± 0.22 Ma (Table S1,† Fig. 3). The four older dates are statistically equivalent with a weighted mean of 417.45 ± 0.11 Ma (MSWD = 0.73). We attribute the single resolvable younger date to residual Pb-loss. The five aliquots with Pb measured in static mode yielded statistically indistinguishable Th-corrected $^{206}Pb/^{238}U$ dates with a weighted mean of 417.310 ± 0.074 Ma (MSWD = 1.8), which is in excellent agreement with the SEM data (Fig. 3). The weighted mean dates of both datasets are significantly older than the originally recommended date of 416.78 ± 0.33 Ma (ref. 17). This is likely related to residual Pb-loss in the Black *et al.*[17] data, due to the fact that their samples were not pre-treated by a CA-technique.[11] However, our data are in excellent agreement with a more recently published date of 417.43 ± 0.06 Ma (ref. 18) that was measured using the same tracer solution employed in this study and thus are comparable at the level of analytical uncertainties.

Again, the excellent agreement between our two datasets as well as published reference data suggests accurate calibration of

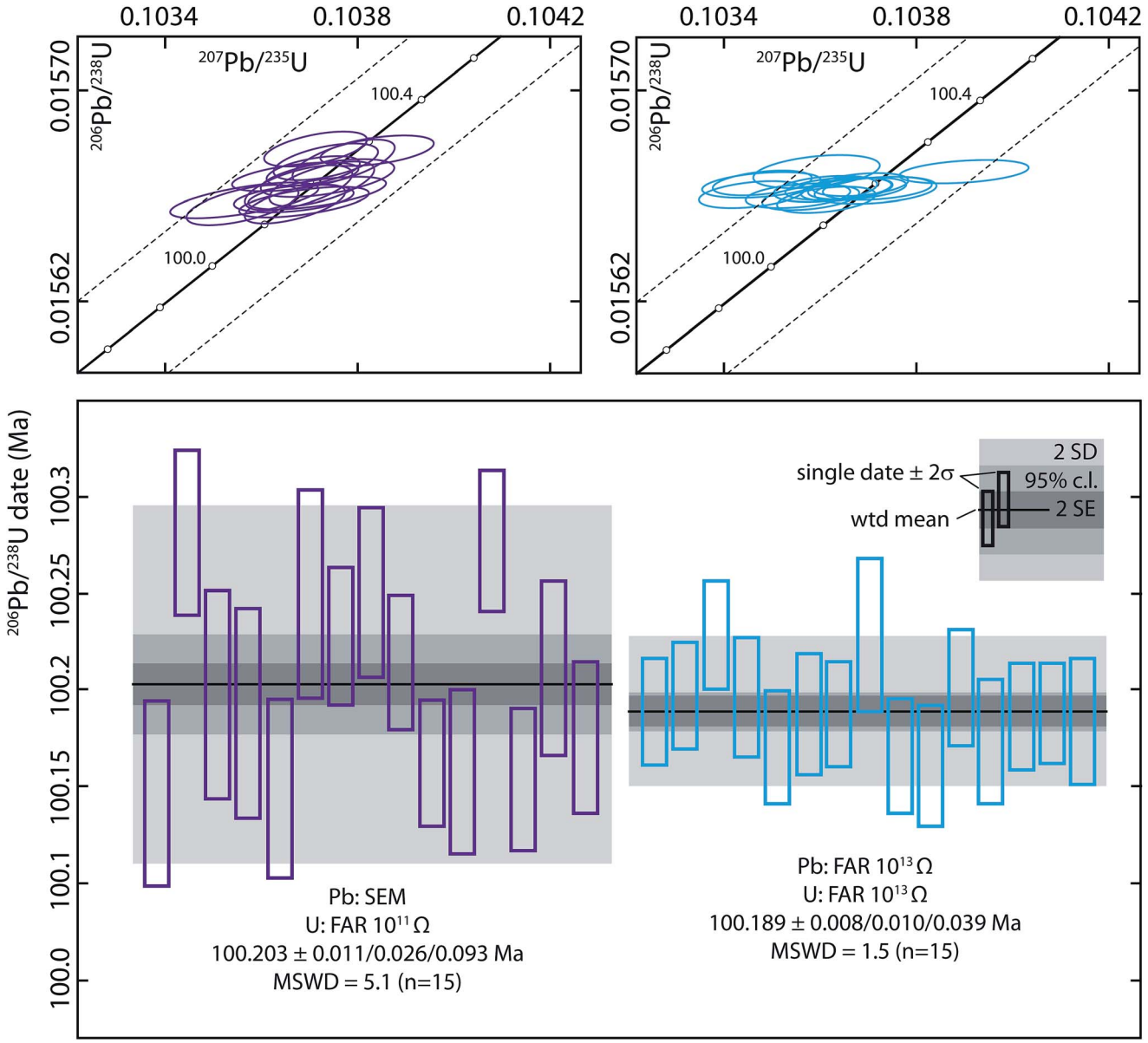

Fig. 2 U–Pb systematics of repeated analyses of ET100 synthetic solution. (Top) $^{206}Pb/^{238}U$ and $^{207}Pb/^{235}U$ systematics shown in concordia space. Uncertainty in the position of the concordia arises from the uncertainties in the U decay constant and is shown as dotted lines. (Bottom) $^{206}Pb/^{238}U$ dates with 2σ analytical uncertainties for SEM and FAR measurements. Individual dates for each detector setup are ordered by the run number. Horizontal bars are weighted mean dates with uncertainties shown at 2 SE, 95% confidence interval and 2 SD. These uncertainties are also given numerically as *X*/*Y*/*Z*, with *X* being 2 SE, *Y* being the 95% confidence interval and *Z* being 2 SD – (see the text for details). MSWD – mean square of weighted deviates.

the two detector systems. Notably, the static Pb measurements were run for approximately 90 minutes while SEM measurements were run for more than three hours. Another advantage of the static Faraday measurements is the significantly extended dynamic range, allowing measurements at higher intensity for such Pb* rich zircons. Zircons of comparable age and U content can produce ^{206}Pb signals well beyond the linear range of the SEM (>20 mV relative to 10^{11} ohm resistor) at typical run temperatures of 1220–1270 °C (Fig. 5). The two possibilities to run such samples on the ion counting system are to either reduce the operating temperature, which increases the possibility of collecting isobaric interferences on ^{204}Pb and ^{207}Pb, or to significantly burn off the sample before switching to the ion counting system (or a combination of both). In each case, the less abundant ^{204}Pb, ^{207}Pb and ^{208}Pb as well as the tracer masses ^{202}Pb and ^{205}Pb will have significantly lower intensities leading to lower precision U/Pb and Pb/Pb ratios. Such zircon materials with a high ^{206}Pb signal as well as high-Th minerals such as monazite ($CePO_4$) with high ^{208}Pb intensities are particularly suitable for static Faraday measurements using the new 10^{13} ohm amplifiers.

AUS_Z7_5. AUS_Z7_5 is a 2.4 Ma zircon from a suite of gem quality crystals from New South Wales, Eastern Australia, similar to those characterised by Kennedy *et al.*[19] This particular

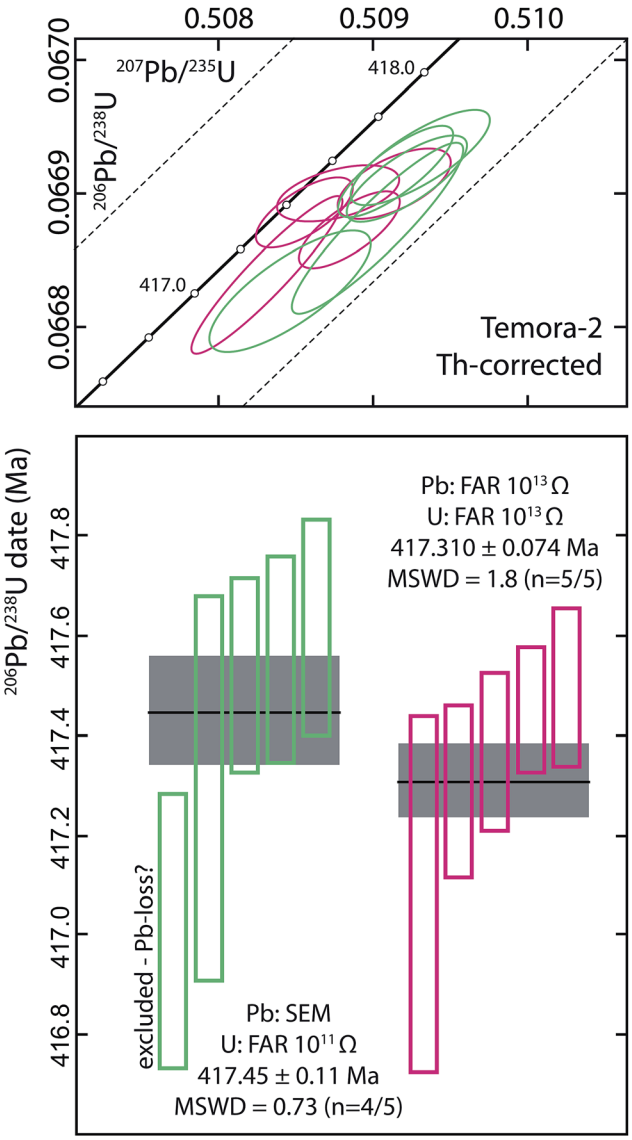

Fig. 3 U–Pb systematics of repeated analyses of the Temora-2 zircon standard. (Top) $^{206}Pb/^{238}U$ and $^{207}Pb/^{235}U$ systematics shown in concordia space. Uncertainty in the position of the concordia arises from the uncertainties in the U decay constant and is shown as dotted lines. (Bottom) Ranked $^{206}Pb/^{238}U$ dates with 2σ analytical uncertainties for SEM and FAR measurements. Horizontal bars are weighted mean dates with uncertainties shown at 2σ. MSWD – mean square of weighted deviates.

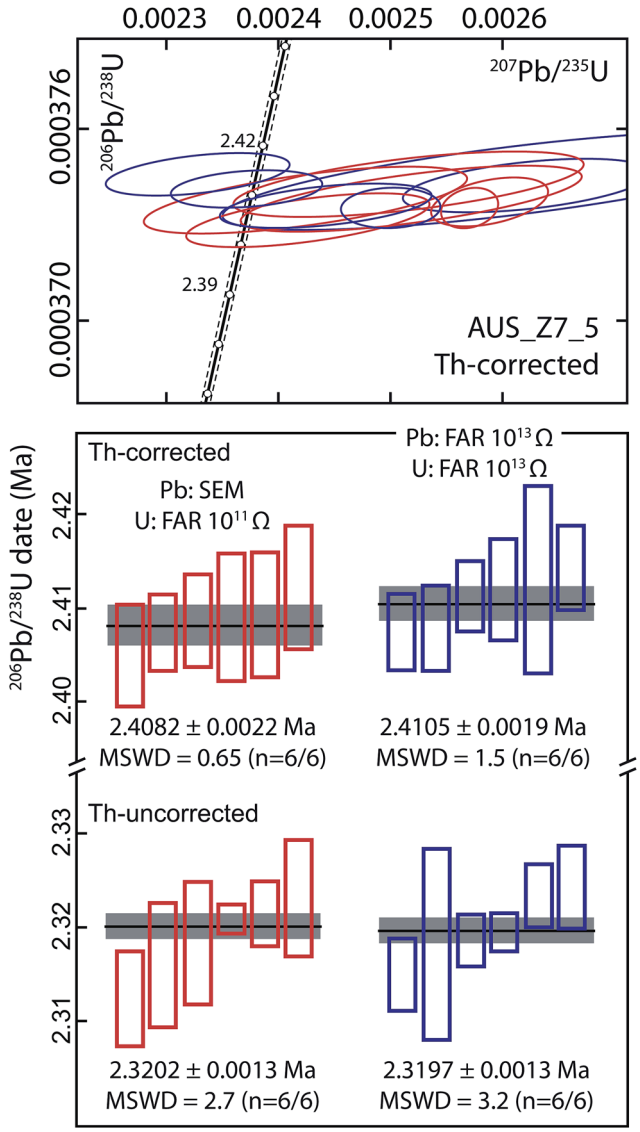

Fig. 4 U–Pb systematics of repeated analyses of the AUS_Z7_5 zircon standard (Top) $^{206}Pb/^{238}U$ and $^{207}Pb/^{235}U$ systematics shown in concordia space. Uncertainty in the position of the concordia arises from the uncertainties in the U decay constant and is shown as dotted lines. (Bottom) Ranked $^{206}Pb/^{238}U$ dates with 2σ analytical uncertainties for SEM and FAR measurements. Shown are both ^{230}Th disequilibria corrected and uncorrected $^{206}Pb/^{238}U$ dates. Horizontal bars are weighted mean dates with uncertainties shown at 2σ. MSWD – mean square of weighted deviates.

crystal was previously characterised by LA-ICP-MS at ETH Zurich as an in-house secondary standard. We here use this zircon to evaluate the performance of our static Faraday routine at low ion beam intensities and low Pb*/Pb_c ratios where baselines and yield stability are particularly important.

Six fragments with Pb* between 0.576 and 3.93 pg were analysed using dynamic ion counting for Pb and six fragments with Pb* between 0.551 and 2.33 pg were analysed using static Faraday collection with 10^{13} ohm resistors (Table S1†). Fig. 4 compares the results of the two detector setups in concordia space (corrected for initial ^{230}Th disequilibrium) and as ranked single crystal $^{206}Pb/^{238}U$ dates and their weighted means (both corrected and uncorrected for initial ^{230}Th disequilibrium). Six analyses using the SEM for Pb yielded a weighted mean $^{206}Pb/^{238}U$ date of 2.3202 ± 0.0013 Ma. Six analyses using the static routine for Pb yielded a weighted mean of 2.3197 ± 0.0013 Ma, in excellent agreement with the SEM data.

For both detector setups, these ^{230}Th-uncorrected $^{206}Pb/^{238}U$ dates show some dispersion in excess of what is expected from analytical scatter with MSWDs of 2.7 and 3.2, respectively, suggesting that the AUS_Z7_5 zircon is not perfectly homogeneous (Fig. 4). Applying a ^{230}Th-correction using an assumed Th/U of the magma of 3.0 ± 0.5 (2σ) results in Th-corrected

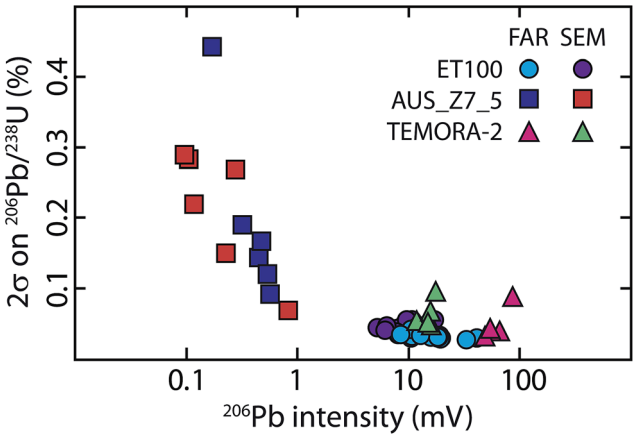

Fig. 5 Uncertainty on the $^{206}Pb/^{238}U$ ratio (corrected for fractionation, tracer and blank) as a function of ^{206}Pb beam intensity (in mV) for samples analyzed in this study (normalized to a 10^{11} ohm current amplifier). See the text for details.

weighted mean $^{206}Pb/^{238}U$ dates of 2.4082 ± 0.0022 Ma (MSWD = 0.65) and 2.4105 ± 0.0019 Ma (MSWD = 1.5). These data again demonstrate the excellent agreement between the two detector systems.

In contrast to the $^{206}Pb/^{238}U$ dates, both datasets show significant dispersion in the $^{207}Pb/^{235}U$ ratio, with a systematic shift to higher $^{207}Pb/^{235}U$ relative to concordia (Fig. 4). This systematic shift and dispersion can be caused by analytical effects such as inaccuracies in the blank composition or isobaric interferences on ^{207}Pb and ^{204}Pb, but can also result from initial ^{231}Pa disequilibria in the ^{235}U–^{207}Pb decay chain.[7,20,21] We are confident that our blank composition is accurate within uncertainty and many of the analyses are too radiogenic ($^{206}Pb/^{204}Pb$ up to >2000) to explain the discordance with inaccurate blank corrections. Isobaric interferences on ^{207}Pb and ^{204}Pb are common in radiogenic Pb TIMS analyses and we often observe changes in ratios involving these isotopes at the beginning of analyses. However, interfering organic molecules usually burn off within 1–2 blocks during ion counting measurements and all ratios remain constant over the remaining 2–3 hours of data collection. Under similar run conditions, these isobaric interferences could be present for longer during the faster static Faraday measurements. However, we usually run static Pb measurements at slightly higher temperatures and only occasionally observe minor effects of isobaric interferences at the beginning of these measurements after which all ratios remain constant. We therefore are confident that the systematic discordance is not due to isobaric interferences but rather results from initial ^{231}Pa excess, a conclusion also reached by ref. 19 for older zircons from the same suite of gem crystals. We note, however, that the dispersion in $^{207}Pb/^{235}U$ is slightly larger for our static Faraday measurements, compared to our SEM analyses. This may indeed be an analytical artefact related to instabilities in the SEM ion yield and/or amplifier baselines in excess of what we observed based on repeated measurements of these instrumental parameters over the course of this study.

The AUS_Z7_5 data also allow the assessment of the lower limit in terms of signal intensity that still produces sufficiently precise and accurate Pb/Pb and U/Pb ratios. For the Faraday measurements, the average ^{206}Pb intensity ranged from 0.172 to 0.572 mV (relative to the 10^{11} ohm amplifier gain; Fig. 5). At this intensity the within-run precision of the $^{206}Pb/^{205}Pb$ ratio and the precision of the final $^{206}Pb/^{238}U$ ratio are comparable between SEM and static Faraday measurements (Fig. 5). The less abundant isotopes ^{207}Pb and ^{208}Pb yielded average signal intensities of 25–40 μV and 63–137 μV (relative to the 10^{11} ohm amplifier gain), respectively. At such low intensities the within-run precision of the $^{207}Pb/^{205}Pb$ and $^{208}Pb/^{205}Pb$ ratios is significantly more precise for the SEM measurements compared to the Faraday measurements. These lower precision measurements of the minor Pb isotopes, however, only have limited impact on the uncertainties of calculated U–Pb dates. In the case of $^{207}Pb/^{235}U$ dates, this is because the uncertainties are entirely dominated by uncertainties associated with the blank correction (*i.e.*, the uncertainty on the $^{207}Pb/^{204}Pb$ of the blank). For $^{206}Pb/^{238}U$ dates, the ^{208}Pb is important for the model calculation of the Th/U of the respective zircon that is then used in the initial ^{230}Th disequilibria correction. The lower precision $^{208}Pb/^{205}Pb$ and $^{206}Pb/^{208}Pb$ measurements however contribute less than 0.5% to the uncertainty in the Th/U and thus are not a significant source of uncertainty in the Th-correction.

We therefore conclude that our static measurement routine with 10^{13} ohm resistors produces precise and accurate U–Pb results, even for zircons with Pb* of less than 1 pg that yield ion beam intensities of <1 mV for ^{206}Pb and <0.04 mV for ^{207}Pb, respectively (normalised to the 10^{11} ohm amplifier gain).

Conclusions and outlook

We investigated the performance of new 10^{13} ohm resistors installed in a Thermo TRITON Plus TIMS instrument to measure Pb/Pb and U/Pb ratios in small samples (<1 to 700 pg) with static collection of all natural and tracer Pb isotopes ($^{202,204,205,206,207,208}Pb$). U–Pb dates of natural and synthetic standard materials collected using this static measurement routine are compared to U–Pb data with Pb measured by conventional dynamic ion counting.

Our analyses reveal excellent agreement between the two detector setups for all analysed standards. Repeated analyses of synthetic U–Pb solution aliquots suggest that the static Faraday measurements are a factor of 2–3 more reproducible compared to our SEM measurements.

The advantages of the larger linear range of Faraday cups are demonstrated by analyses of Pb*-rich Temora-2 standard zircons. For these zircons, the within-run precision of Pb isotope ratios is 2–5 times more precise for the Faraday measurements compared to SEM measurements. Uncertainties of final U–Pb ratios and derived U–Pb dates, however, are only slightly reduced (Fig. 5) due to external sources of uncertainty.

For high-Pb* samples comparable to the ET100 solution and Temora-2, the most significant source of uncertainty is associated with the correction for U-oxide interferences. The uncertainty in the $^{18}O/^{16}O$ ratio used in this correction accounts for

up to 60% of the uncertainty of $^{206}Pb/^{238}U$ dates in our datasets. This source of uncertainty can almost entirely be eliminated by directly measuring the $^{18}O/^{16}O$ ratio during the U measurement. This requires collecting the $^{238}U^{18}O^{16}O$ ($^{272}UO_2$) isotopologue in the axial ion counter along with precise determinations of the SEM ion yield for U. Eliminating this source of uncertainty would significantly increase the benefit of the improved precision of the Faraday measurements.

Low-U, young and thus unradiogenic zircons with Pb* <1 pg were successfully measured using our static routine, demonstrating the stability of amplifier baselines and SEM ion yield. For such unradiogenic zircons, the SEM measurements of the minor ^{207}Pb and ^{208}Pb isotopes are more precise than the Faraday measurements but this has only minor impact on the precision of U–Pb dates.

The results of this study suggest that the new 10^{13} ohm resistors of the Thermo Scientific™ TRITON™ Plus instrument allow precise and accurate static Faraday measurements of radiogenic Pb for accessory mineral U–Pb geochronology. We anticipate that this will be a crucial advancement in the quest towards inter- and intralaboratory reproducibility at the 0.01% level and will allow more precise and accurate quantification of the timing, rates and durations of geological processes and events.

Appendix

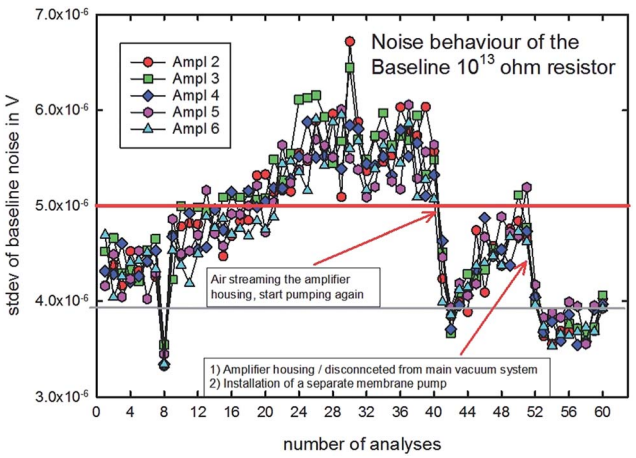

Fig. 6 Long-term measurement of the baseline noise for the new 10^{13} ohm amplifiers expressed as the standard deviation of one hour baseline measurements. Each individual data point represents a one hour measurement.

Acknowledgements

This work was supported by the D-ERDW of ETH Zurich. J. F. W. acknowledges support through the ETH Zurich Postdoctoral Fellowship Program; Y. B. and S. L. were supported through the SNF project 200021-146651. The authors thank two anonymous reviewers for constructive comments.

Notes and references

1 B. Schoene, in *Treatise on Geochemistry*, ed. H. D. H. K. Turekian, Elsevier, Oxford, 2nd edn, 2014, pp. 341–378.
2 Y. Amelin and W. J. Davis, *Geochim. Cosmochim. Acta*, 2006, **70**, A14.
3 D. J. Condon, B. Schoene, N. M. McLean, S. A. Bowring and R. R. Parrish, *Geochim. Cosmochim. Acta*, 2015, **164**, 464–480.
4 N. M. McLean, D. J. Condon, B. Schoene and S. A. Bowring, *Geochim. Cosmochim. Acta*, 2015, **164**, 481–501.
5 B. Schoene, J. Guex, A. Bartolini, U. Schaltegger and T. J. Blackburn, *Geology*, 2010, **38**, 387–390.
6 T. J. Blackburn, P. E. Olsen, S. A. Bowring, N. M. McLean, D. V. Kent, J. Puffer, G. McHone, E. T. Rasbury and M. Et-Touhami, *Science*, 2013, **340**, 941–945.
7 J. F. Wotzlaw, S. K. Hüsing, F. J. Hilgen and U. Schaltegger, *Earth Planet. Sci. Lett.*, 2014, **407**, 19–34.
8 J. M. Koornneef, C. Bouman, J. B. Schwieters and G. R. Davies, *Anal. Chim. Acta*, 2014, **819**, 49–55.
9 M. Klaver, R. J. Smeets, J. M. Koornneef, G. R. Davies and P. Z. Vroon, *J. Anal. At. Spectrom.*, 2015, **31**, 171–178.
10 D. J. Condon, N. M. McLean, B. Schoene, S. A. Bowring, R. Parrish and S. Noble, *Geochim. Cosmochim. Acta*, 2008, **72**(12S), A175.
11 J. M. Mattinson, *Chem. Geol.*, 2005, **220**, 47–66.
12 A. Trinquier, *Thermo Scientific, Technical Note 30285*, 2014.
13 J. Hiess, D. J. Condon, N. M. McLean and S. R. Noble, *Science*, 2012, **335**, 1610–1624.
14 J. F. Bowring, N. M. McLean and S. A. Bowring, *Geochem., Geophys., Geosyst.*, 2011, **12**, Q0AA19, DOI: 10.1029/2010GC003479.
15 N. M. McLean, J. F. Bowring and S. A. Bowring, *Geochem., Geophys., Geosyst.*, 2011, **12**, Q0AA18, DOI: 10.1029/2010GC003478.
16 A. H. Jaffey, K. F. Flynn, L. E. Glendenin, W. C. Bentlea and A. M. Essling, *Phys. Rev. C: Nucl. Phys.*, 1971, **4**, 1889–1906.
17 L. P. Black, S. L. Kamo, C. M. Allen, D. W. Davis, J. N. Aleinikoff, J. W. Valley, R. Mundil, I. H. Campbell, R. J. Korsch, I. S. Williams and C. Foudoulis, *Chem. Geol.*, 2004, **205**, 115–140.
18 V. I. Davydov, J. L. Crowley, M. D. Schmitz and V. I. Poletaev, *Geochem., Geophys., Geosyst.*, 2010, **11**, Q0AA04, DOI: 10.1029/2009QC002736.
19 A. K. Kennedy, J. F. Wotzlaw, U. Schaltegger, J. L. Crowley and M. Schmitz, *Can. Mineral.*, 2014, **52**, 409–421.
20 A. K. Schmitt, *Am. Mineral.*, 2007, **92**, 691–694.
21 M. Rioux, S. A. Bowring, M. Cheadle and J. Barbara, *Chem. Geol.*, 2015, **397**, 143–156.